Entropic sampling of flexible polyelectrolytes within the Wang-Landau algorithm

N. A. Volkov and P. N. Vorontsov-Velyaminov*
Faculty of Physics, St. Petersburg State University, 198504, St. Petersburg, Russia

A. P. Lyubartsev†
Division of Physical Chemistry, Arrhenius Laboratory, Stockholm University, S-10691, Stockholm, Sweden
(Received 7 February 2006; revised manuscript received 6 September 2006; published 11 January 2007)

We extend the Monte Carlo methods developed in our previous papers [J. Phys. A **37**, 1573 (2004); Macromol. Theory-Simul. **14**, 491 (2005)] and based on entropic sampling within the Wang-Landau algorithm to simulation of a lattice model of flexible polyelectrolytes. We consider a strongly charged polyelectrolyte chain accompanied by neutralizing counterions on a simple cubic lattice with periodic boundary conditions. The Coulomb potential and the excluded volume condition between different ions or beads are taken into account. The obtained energy distributions make possible the calculation of canonical properties such as conformational energy, heat capacity, entropy, free energy, and mean-square end-to-end distance over a wide temperature range in a single simulation.

DOI: 10.1103/PhysRevE.75.016705 PACS number(s): 05.10.Ln, 05.20.Gg, 82.35.Rs

I. INTRODUCTION

Many biologically important macromolecules as well as synthetic polymers dissociate in solution, forming charged polyions surrounded by an atmosphere of mobile ions. Electrostatic interactions play a very important role in the behavior and functioning of biological polyelectrolytes. The ability of polyelectrolytes to change their sizes greatly upon change of ionic conditions and temperature makes them interesting in many technological applications.

Theoretical description of flexible polyelectrolytes is a very difficult problem. There exist theories that describe uncharged polymer chains, but they are generally not applicable to description of polyelectrolytes because of the long-range character of the electrostatic interactions. At best, interactions between monomers of polyions can be described by a Debye-Hückel approximation, without explicit presentation of counterions. For strongly charged polyelectrolyte solutions, however, there is no clear understanding of even the most fundamental scaling properties. So computer simulation has become an indispensable tool for investigating such systems [1].

The number of computer simulation works on flexible polyelectrolytes with explicit account of counterions is still limited [2–5]. In recent years a series of new works in this area have appeared [6–9], but there are still many open questions to be considered. One of the problems is declining efficiency of the standard simulation techniques when the strength of the electrostatic interactions is increased or the effective temperature becomes low. Another issue of interest is the free energy which is closely related to the experimentally observed properties of molecular systems. The main difficulty in its calculation is that free energy cannot be obtained by simple averaging over the generated configurations of the system, because it is a property of the whole statistical ensemble. That is why one has to use specific methods to calculate the free energy of the polyelectrolyte system, in order to be able to make comparisons with experiment.

Generalized ensemble Monte Carlo (MC) methods developed during the past decade [10–12] have proved to be efficient in simulation of highly nonideal molecular systems, e.g., in treatment of systems having rough multiminima potential landscapes, and phenomena occurring at low temperatures and high densities [13–15]. One of these advanced techniques is entropic sampling (ES) within the Wang-Landau (WL) algorithm, suggested in 2001 in papers [16,17]. It is important to note that the latter method is rather general and can be readily applied to molecular systems of very different kinds. Indeed, since 2002 the ES-WL technique has been used by many groups to study fluids [18,19], glasses [20], collapse of polymer chains [21], proteins [22–24], and other molecular systems (see, e.g. [25–27]).

In our previous works [28,29] we applied the WL algorithm to ES simulation of free and ring polymer chains on a three-dimensional simple cubic lattice. For short lattice chains our numerical results were tested by comparison with the exact data. For an athermal lattice model the existing scaling relations, such as the N dependence of the number of self-avoiding walks and the mean-square end-to-end distance, were well reproduced in the range of chain lengths up to $N=1000$ [29]. In the thermal case we calculated distributions over the number of monomer contacts. The distributions were used for obtaining canonical (thermal) averages—conformational energy, heat capacity, entropy, mean-square end-to-end distance, and expansion factor. Our thermal data for the energy agreed well with simulation results of other authors, obtained earlier with different algorithms [30,31].

The aim of the present study is to develop the ES-WL approach for flexible polyelectrolyte systems with explicit ions, and to address some important problems in polyelectrolyte theory. Our primary interest is temperature and polymer length dependence of the thermodynamical properties (energy and free energy) as well as the average size of the polyelectrolyte chains. It is well recognized in the theory of noncharged polymers that such fundamental properties of

*Electronic address: voron.wgroup@pobox.spbu.ru
†Electronic address: sasha@physc.su.se

polymer solutions depend weakly on details of the model and can be understood within lattice models. Lattice models are more convenient from the simulation point of view. Therefore in the present study we consider the polyelectrolyte on a lattice.

The plan of the paper is as follows. In Sec. II we discuss the model of the polyelectrolyte and the method of simulation, i.e., the general idea of entropic sampling within the WL algorithm and some modifications of the method. The obtained results and their treatment are given in Sec. III. Section IV contains final remarks.

II. MODEL AND METHOD OF CALCULATION

A. Model

In this study we consider a lattice model of a polyelectrolyte that was previously studied in our earlier paper [2]. The polyion is presented as a chain on a simple cubic lattice with periodic boundary conditions. The chain consists of N_p successive beads (monomers) connected by rigid bonds of unit length. Each monomer of the chain carries a unit negative electric charge. Because counterions of the opposite sign are necessarily present in any real system to provide electroneutrality, an appropriate number of them is added. Each mobile ion is represented by a single bead which occupies one of the lattice sites. Counterions are located on a lattice shifted by a vector $(0.5;0.5;0.5)$ relative to the lattice occupied by the polyion. Such a shift of the mobile ion sublattice makes the MC procedure more efficient by eliminating the possibility of overlaps of the mobile ions with the polyion. In order to satisfy the excluded volume condition, the beads of the chain cannot overlap (self-avoiding polymer). That is also true for the mobile ions. However, as long as we use the WL algorithm for our simulations, self-intersections of the chain and overlaps of the mobile ions are allowed in the course of simulations, and are then accounted for in a proper way. The details of this procedure are described in the next section.

The volume (number of sites) of the simulation cell for each lattice is $V=L^3$, where L is the side length of the cell. In our calculations we considered polyions of length $N=10,30,50$, and 80 bonds ($N_p=11$, 31, 51, and 81 correspondingly). In the case of absence of added salt conformational properties of polyelectrolytes are defined by two independent parameters, which may be expressed as a concentration of polyions (which is determined by the volume of the system) and a concentration of small ions (which is equal to the concentration of the monomers). We therefore carried out two series of calculations. In the first one the specific volume per polyion was kept constant, and in this case the side length of the cell was the same for all N, $L=30$. The volume fraction per monomer, $c_p=N_p/V$, in this case ranged from 4.07×10^{-4} for $N_p=11$ to 3×10^{-3} for $N_p=81$. The volume fraction of the counterions, c_i, is equal to that of monomers, c_p. In the second series we kept constant the volume fraction per monomer and took it to be equal to that for $N_p=11$ of the first series, i.e., $c_p=4.07\times10^{-4}$. So for $N_p=11$ the side length of the cell was the same as before, $L=30$. For $N_p=31,51,81$ it was $L=42,50,58$, respectively.

Note that in some of our simulations the length of the polyion exceeds the simulation box size, so that the polyion can in some configurations contact a periodic image of itself. This can be interpreted as modeling of a finite polyion concentration when periodic images mimic neighboring polyions.

Both polyelectrolyte monomers and mobile ions interact by Coulombic potential $V(r)=q_iq_j/r$, where q_i are charges of the corresponding species ($q_i=\pm q$; $q>0$). The natural units for our model are the lattice constant a and the charge q. So the energy is measured in q^2/a units and the temperature in q^2/ak_B. Remembering the definition of the reduced polyion charge density ξ as the ratio of the Bjerrum length (distance at which the energy of interaction of unit charges is equal to the thermal energy) to the charge spacing along the polyion, we can conclude that $\xi=1/T$ in the adopted units. Thus the correspondence is established between the reduced temperature T of our model and the parameter ξ, the characteristic of real polyelectrolytes.

A correct treatment of the long-range electrostatic interactions is of great importance for simulations of polyelectrolytes. It is generally accepted that the Ewald summation [32,33] is the most consistent way to treat them, although the possibility of artifacts due to artificial periodicity introduced by the Ewald summation is still debated [34]. We compared Ewald summation results with the data obtained within the minimal image convention. Our test simulations for shorter polyion chains $N_p=11,31$ showed that the minimum image approach gives results practically coinciding with the Ewald summation for the density of energy states of the system [see Figs. 1(a) and 1(b)]. For the polyelectrolyte with $N_p=11$, a small difference between the distributions obtained by these two approaches is observed in a very small area of high energies, which can slightly affect high-temperature properties of the system. For $N_p=31$ the distributions coincide almost completely. For longer chains, simulated with a larger number of ions, the screening is stronger and the difference between these distributions is not supposed to be greater. Note also that the minimum image convention explicitly includes the interactions between all the particle pairs in the system, which removes in fact most of the shortcomings of the simple spherical electrostatic cutoff scheme with small cutoff distance that is sometimes used in biomacromolecular simulations. Using an Ewald summation over periodic images seems natural for systems with inherently repeating nonuniform charge distribution (DNA in crystalline solution, multilammelar membranes) but the advantages of an Ewald summation for treatment of an isolated macromolecule are not so obvious. Taking also into account the fact that the minimum image approach in our case works much faster than the Ewald sum, we used the minimal image approach in most of our productive runs.

B. Method

The aim of our studies is to obtain the density of energy states $\Omega(E)$ for the investigated system. This function can then be used to compute canonical averages in a wide range of temperatures by simple integration. Free energy and en-

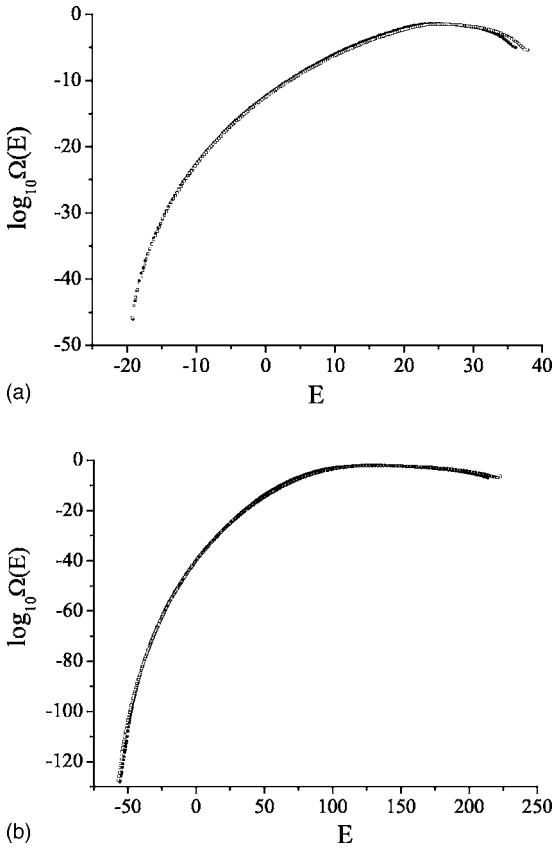

FIG. 1. Normalized distributions $\Omega(E)$ for a polyelectrolyte, obtained by the minimum image convention (empty squares) and by the Ewald method (filled circles); (a) $N_p=11$ and (b) $N_p=31$.

tropy can be obtained from the density of states as well.

We mostly use the same method as in our previous works [28,29], i.e., entropic sampling [11,12] within the WL algorithm [16,17], with some modifications described below. We consider a configurational space of the system consisting of all possible configurations, including overlapping ones. Each nonoverlapping configuration can be characterized by a certain energy, which we assume to be in the range between $\tilde{E}_{\min}$ and $\tilde{E}_{\max}$. This range of energies is divided into a finite number of equal small intervals (bins or discrete states), so that each nonoverlapping configuration belongs to one of them. The number of energy bins in our calculations ranged from about 100 to 1000 depending on N_p. $\tilde{E}_{\min}$ was chosen for each N such that no configurations fall into a number of states close to $\tilde{E}_{\min}$. So the extreme left state which was still visited during a simulation corresponds to an observed minimum energy $E_{\min} \geq \tilde{E}_{\min}$. The attained $E_{\min}$ can be considered as our estimate of the classical ground state of the system.

In principle $\tilde{E}_{\max}$ could be chosen in the same way, so that during a simulation no configurations assume an energy higher than $\tilde{E}_{\max}$, and a few bins remain empty on the right-hand side of the energy range. Actually, since very high energy states are not important for calculating canonical properties at finite $T>0$, we use another (a more economic) scheme at the right side: $\tilde{E}_{\max}$ is chosen to be slightly lower than the actual $E_{\max}$, which for our further calculations is unimportant. For all nonoverlapping states with energy $E>\tilde{E}_{\max}$ a single bin is assigned.

Another set of bins is introduced for overlapping configurations. In principle, we can use one single bin for all overlapping states and get its normalized weight during calculation. However, as clearly shown by our previous work [28], such an approach is not stable, and hence it is necessary to introduce a scheme with a set of bins for overlaps. Each of them corresponds to configurations with a certain number of overlaps of the polyion's beads and of the free ions. The number of bins in this set depends on the length of the polyion and is taken to be in the range 10–100. Every possible number of overlaps less than this boundary value is associated with a separate bin, and one additional bin is used for the number of overlaps exceeding it.

Each configuration of the simulated system can have either a definite number of overlaps or, if no overlaps occur, have a definite energy. Thus any configuration of our system can be attributed to one of the bins of the first or second type. During simulation we count the number of states corresponding to each bin, which can then be converted into the fraction of nonoverlapping configurations Ω_0, the fraction of all overlapping configurations $1-\Omega_0$, and the normalized density of states $\Omega(E)$ taken over nonoverlapping configurations only.

We perform a random walk in the whole configurational space according to the WL procedure. As in previous works [28,29], it is convenient to introduce the entropy distribution $S_i=\ln \Omega_i$ (initially all $S_i=0$). Two sets of counters are introduced: One accumulates S_i for each bin (entropy counter); another one, n_i, counts visits to the corresponding states yielding at the end of the run the normalized visit probabilities p_i (the histogram). The aim is to achieve a flat distribution, p_i, over all the states.

A MC step includes a standard trial change of the state with a uniform coordinate distribution. For our polyelectrolyte model, two kinds of steps are performed: We modify the chain's conformation or move a mobile ion. The probability of each kind of step was taken to be 50%. In order to change the position of a randomly chosen ion we make a shift $\pm\Delta$ along one of the axes X, Y, or Z, with $\Delta=1,2,3$. In order to change the conformation of the chain we perform steps of three different types.

(1) We choose homogeneously one of the beads from 0 to N_p-l (e.g., the kth) and change randomly the directions of chain links between beads k and $k+l$. The remaining piece undergoes a parallel shift. Because we do not want to change the energy of the system strongly in a single step, the trajectory displacement should be small. That is why in most of our calculations l was taken equal to 1 so that the change of the conformation was not large.

(2) If by a random choice we find two neighboring perpendicular segments, we change their directions so that the new direction of the first segment is the former direction of the second one and vice versa (the so called Γ move).

(3) Reptation of the chain is also used: We cut off a segment from one end of the chain (which is chosen randomly) and build a new one at the opposite end in a random direction.

The fractions of steps (1), (2), and (3) were 50%, 40%, and 10% respectively.

The trial steps are accepted with the following transition probability condition [16,17]:

$$p(i \to i') = \min[1, \exp(S_i - S_{i'})]. \quad (1)$$

If this condition is fulfilled, the trial state (i') is accepted, and in the opposite case the accepted one is the initial state (i). Finally, the entropy of the accepted state (S_i or $S_{i'}$) is augmented by ΔS, and the corresponding counter of visits (n_i or $n_{i'}$) is increased by 1.

A series of such elementary steps constitute a sweep. According to the original WL algorithm [16,17], at the end of a current sweep ΔS had to be decreased: $\Delta S \to c\Delta S$ by a factor $0 < c < 1$ (in [16] $c=0.5$, and the initial value $\Delta S=1$ was used). After several sweeps the S_i dependence is formed and fine-tuned in the whole range of configurations. At the same time, the probability distribution of visits becomes flat, with probabilities p_i equal to the inverse of the number of bins.

In this work we introduced slight modifications in this simulation technique. We use a factor $c=0.9$ instead of the value $c=0.5$ used in the majority of previous works implementing the WL algorithm. The reason for increasing this factor is that in order to reach configurations with extremely low probability, one needs to accumulate a rather large entropy difference between states of low and high probabilities, which is difficult to get if the increment of the entropy, ΔS, decreases twice after each sweep. With a factor of $c=0.9$ we have to perform more sweeps to reach values of ΔS small enough for fine-tuning the distribution over energies $\Omega(E)$; however, this enables us to attain energy states having extremely low probability (down to 10^{-285}).

Within the WL algorithm the probability of transition to a new state is small if the current state is rare in comparison with the trial one, and vice versa. That is the key point in obtaining statistics for the states with low probabilities. But it can also cause certain problems. If the system drops into some newly found state after many sweeps, it is not able to get out of it until the corresponding quantity S_i becomes large enough and the probability of transition becomes appropriate. The ΔS value decreases in every following sweep according to the WL algorithm. But if, after many sweeps, ΔS is small and $S_i=0$ for a newly visited state, then S_i cannot reach the necessary magnitude comparable with that of previously visited states, and the system gets stuck in that state. The problem of such "holes" was previously considered by Tröster and Dellago [35] for the case of an Ising model. Here we introduce another modification to solve this problem. We consider separate ΔS values for such states, contrary to the usual WL algorithm where quantities ΔS are the same for all the states. If the system has not visited some states during the present sweep we do not change the corresponding value of ΔS, whereas all visited states assume values of $\Delta S = c^n$, n being the sweep number. That is how ΔS for a newly visited state remains large enough and an appropriate value of S_i for this state can be accumulateted faster.

The number of MC steps in the first sweep was 10^6. In order to increase the precision of the energy distribution in the course of tuning the entropy, the number of steps in each subsequent sweep was increased by multiplying the previous number by 1.03. In all cases the used number of steps was sufficient to achieve flatness of the visiting histogram during each sweep. About 120 sweeps were made for each simulated system, though for shorter polymers results became stable after 50–60 sweeps.

Within the procedure described above, the fraction of nonoverlapping configurations Ω_0 can be evaluated as

$$\Omega_0 = \frac{\sum_{k}^{\text{nonoverlap}} \exp(S_k)}{\sum_{l}^{\text{all}} \exp(S_l)}, \quad (2)$$

where the sum in the nominator is taken over bins corresponding to nonoverlapping configurations while a sum in the denominator is taken over all the bins. Similarly, the normalized density of states is calculated as

$$\Omega(E_i) = \frac{\exp(S_i)}{\sum_{k}^{\text{nonoverlap}} \exp(S_k)}. \quad (3)$$

In our calculations Ω_0 ranged approximately from 0.15 for $N_p=11$ to 5.5×10^{-9} for $N_p=81$. These data are presented further in Sec. III. $\Omega(E)$ is calculated rather accurately in a very wide range of orders of magnitude, e.g., from 10^{-1} to 10^{-285} [see Figs. 2(a) and 2(b)]. So the WL algorithm provides calculation probabilities of extremely rare events.

In order to obtain reliable distributions $\Omega(E)$ it is necessary for the system to visit uniformly all possible energy states during a simulation: The histogram at the end of each sweep has to be nearly flat. In Fig. 3 the fraction of visits for each energy state is presented. The data are taken from the simulation of a polyelectrolyte with $N_p=11$ ($\approx 5 \times 10^8$ MC steps). One can see that the relative deviation of the fractions of visits from the average value (inverse of the number of visited energy states) is not greater than 0.4% in almost the whole range of energies. In a rather small area (low energies) the deviation is less than 2%, which is also quite a good result. In Fig. 4 we present the dependency of the energy of the system on the MC time for $N_p=11$ (t denotes the step number). One can see that the system walks many times between points of maximal and minimal energies, and the whole range of energies typical for this polyion length is well covered.

The distribution $\Omega(E_i) \equiv \Omega_i$ obtained within the WL procedure is then used for calculating canonical averages over a wide range of temperatures according to standard relations; e.g., for the internal energy we get

$$\langle E \rangle(T) = \frac{\sum_i E_i \exp\left(-\frac{E_i}{T}\right)\Omega_i}{\sum_i \exp\left(-\frac{E_i}{T}\right)\Omega_i} \equiv \langle E \rangle_{\text{can}}. \quad (4)$$

$\langle E^2 \rangle$ is calculated in the same way, yielding the heat capacity as a function of temperature:

$$C(T) = T^{-2}(\langle E^2 \rangle(T) - [\langle E \rangle(T)]^2). \quad (5)$$

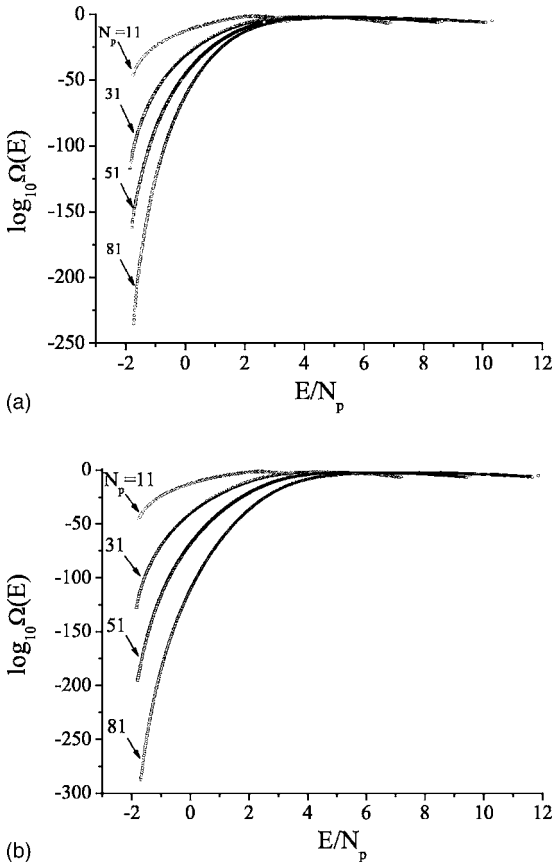

FIG. 2. Normalized distributions $\Omega(E)$ as functions of the specific energy E/N_p for polyelectrolytes of different length. (a) First series of calculations (fixed side length of the cell) and (b) second series (fixed volume fraction per monomer).

In the expression for the energy (4) the normalization of Ω_i is not important, since Ω_i enters both numerator and denominator in Eq. (4) and any constant factor cancels. In order to calculate the free energy we must use instead the quantity $W_{\mathrm{ph}}\Omega_0\Omega_i$, which equals the total number of the system's configurations with the energy E_i satisfying the excluded volume condition. W_{ph} is the number of all possible configurations of the system including overlapping ones (index "ph" stands for "phantom" chains, that is chains allowing overlaps, and phantom ions), Ω_0 is the fraction of configurations without overlaps of ions and polymer beads among all the configurations, and Ω_i is the normalized density of energy states. So for free energy F we have

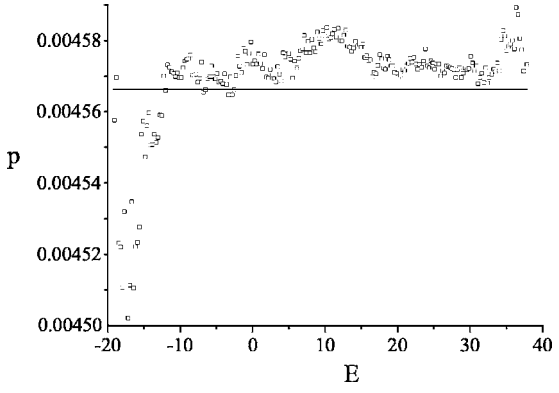

FIG. 3. Rates of visits $p(E)$ (histogram) for $N_p=11$. Solid line indicates predicted level N_b^{-1} (inverse number of energy bins).

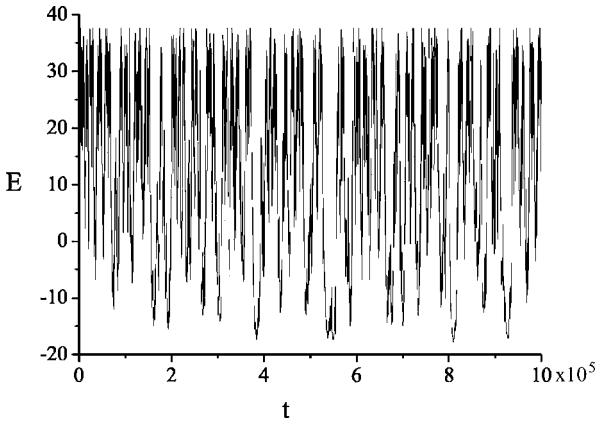

FIG. 4. Dependency of the energy, E, on the number of MC moves, t, in the process of entropic sampling, $N_p=11$.

$$F(T) = -T\ln\sum_i \exp\left(-\frac{E_i}{T}\right) W_{\mathrm{ph}}\Omega_0\Omega_i$$

$$= -T\ln W_{\mathrm{ph}} - T\ln\Omega_0 - T\ln\sum_i \exp\left(-\frac{E_i}{T}\right)\Omega_i. \quad (6)$$

Now the free energy is expressed as

$$F = F_{\mathrm{ph}} + \Delta F_{\mathrm{at}} + \Delta F, \quad (7)$$

where $F_{\mathrm{ph}}=-T\ln W_{\mathrm{ph}}$ is the free energy of a phantom system, $\Delta F_{\mathrm{at}}=-T\ln\Omega_0$ is the excess free energy for the athermal case, and

$$\Delta F = -T\ln\sum_i \exp\left(-\frac{E_i}{T}\right)\Omega_i \quad (8)$$

is the excess canonical free energy (it vanishes in the absence of intereactions).

The canonical entropy $S(T)=[E(T)-F(T)]/T$ can be expressed in a similar way:

$$S(T) = S_{\mathrm{ph}} + \Delta S_{\mathrm{at}} + \Delta S(T), \quad (9)$$

where $S_{\mathrm{ph}}=-(1/T)F_{\mathrm{ph}}=\ln W_{\mathrm{ph}}$, $\Delta S_{\mathrm{at}}=-(1/T)F_{\mathrm{at}}=\ln\Omega_0$, and

$$\Delta S(T) = \frac{E(T)}{T} - \frac{\Delta F(T)}{T} = \frac{E(T)}{T} + \ln\sum_i \exp\left(-\frac{E_i}{T}\right)\Omega_i. \quad (10)$$

For the lattice system consisting of the polyion and N_p counterions the total number of configurations is

$$W_{\mathrm{ph}} = W_{\mathrm{ph1}}W_{\mathrm{ph2}}, \quad (11)$$

where

$$W_{\mathrm{ph1}} = L^3 \times 6^{(N_p-1)} \quad (12)$$

is the number of phantom polyion conformations and

TABLE I. Summary of the results. N_p is the number of beads in the polyion, L is the simulation box length, S_{ph} is the entropy of the phantom system, Ω_0 is the fraction of nonoverlapping configurations, $\Delta S_{at}=\ln \Omega_0$ is the excess entropy for the athermal case obtained within the WL procedure, while ΔS_{at}^{scal} is the same quantity evaluated from scaling relations (14)–(17), T_0 is the temperature of maximum of $\sqrt{\langle R^2\rangle}(T)$, and $\sqrt{\langle R^2\rangle}(T_0)$ is its maximum value.

N_p	L	S_{ph}	Ω_0	ΔS_{at}	ΔS_{at}^{scal}	T_0	$\sqrt{\langle R^2\rangle}(T_0)$
11	30	122.9	0.146	−1.92	−1.94	0.92	5.60
31	30	302.2	0.00121	−6.72	−6.72	1.26	15.04
51	30	467.8	9.00×10^{-6}	−11.62	−11.62	1.44	22.66
81	30	702.0	5.81×10^{-9}	−18.96	−19.04	1.66	31.88
31	42	334.5	0.00123	−6.70	−6.71	1.18	15.94
51	50	547.4	9.19×10^{-6}	−11.60	−11.58	1.28	26.75
81	58	864.1	5.98×10^{-9}	−18.96	−18.94	1.36	40.38

$$W_{ph2}=\frac{L^{(3N_p)}}{N_p!} \tag{13}$$

is the number of ways to place N_p phantom counterions in the cell of volume L^3.

The entropy of a phantom system, defined as $S_{ph}=\ln W_{ph}$ with W_{ph} computed according to Eqs. (11)–(13), is given in Table I for each of the simulated systems.

The fraction of nonoverlapping configurations Ω_0 can be factorized into the ionic and polymer parts:

$$\Omega_0=\Omega_{01}\Omega_{02}, \tag{14}$$

where Ω_{01} is the fraction of polyions without intersections and

$$\Omega_{02}=C_{L^3}^{N_p}/W_{ph2}=\frac{(L^3)!}{(L^3-N_p)!\,L^{3N_p}} \tag{15}$$

is the fraction of configurations without overlaps for the system that consists of the counterions only ($C_{L^3}^{N_p}$ is the binomial coefficient).

Ω_{01} can be predicted theoretically using the scaling relation [30,36] for the number of self-avoiding walks

$$W_N=A\mu^N N^{\gamma-1}, \tag{16}$$

where the length of the walk N equals N_p-1. For the simple cubic lattice, the values of the constants are $\mu=4.6838$, $\gamma=7/6$, and $A=1.17$ [36,37]. Then

$$\Omega_{01}=L^3A\mu^{N_p-1}(N_p-1)^{\gamma-1}/W_{ph1}=A\mu^{N_p-1}(N_p-1)^{\gamma-1}/6^{(N_p-1)}. \tag{17}$$

Ω_{01} is also calculated from Ω_0 obtained in our WL simulations using Eq. (2) (see also [28]). A comparison of these data sets is presented in Sec. III (see Table I).

The excess entropy for the athermal case, $\Delta S_{at}=\ln \Omega_0$, can be estimated from Eqs. (14) and (15). According to relation (8) the canonical contribution ΔF depends on the distribution Ω_i only, and can be easily calculated. One can also obtain $\Delta S(T)$ using the expressions (4) and (10).

For the mean-square end-to-end distance we can calculate the average $\langle R^2\rangle_i$ for each ith bin corresponding to nonoverlapping configurations, $1\le i\le n_E$, within a WL procedure and finally get canonical averages in a standard way similar to Eq. (4):

$$\langle R^2\rangle(T)=\frac{\sum_i \langle R^2\rangle_i \exp\left(-\frac{E_i}{T}\right)\Omega_i}{\sum_i \exp\left(-\frac{E_i}{T}\right)\Omega_i}\equiv\langle\langle R^2\rangle_i\rangle_{can}. \tag{18}$$

III. RESULTS

The key result of our WL calculations is the density of states $\Omega(E)$, which enables us to obtain canonical averages in a wide temperature range. The distributions $\Omega(E)$ for polyelectrolytes in two series of calculations are presented in Figs. 2(a) and 2(b).

As long as we use E/N_p scale for the energy [Figs. 2(a) and 2(b)] it can be seen that the values of specific lowest energies for different polyionic lengths are close to each other: In the first series $E_{min}/N_p\approx-1.754,-1.847,-1.799,-1,734$ for $N_p=11,31,51,81$, respectively; in the second series $E_{min}/N_p\approx-1.754,-1.840,-1.809,-1.695$. We can consider these values attained during the simulation as our estimates of the ground states of our model. Note also that all the obtained specific lowest energies are similar to each other, which means that they depend little on the length of the polyion and on the polyion or monomer concentration.

The dependencies of the specific energy of the system on temperature, $E(T)/N_p$, obtained from Eq. (4), are presented in Figs. 5(a) and 5(b). We also used the Metropolis algorithm to calculate the energy for $N_p=11$ and $N_p=81$ at some temperatures and made comparisons with the corresponding WL results. The two methods show good coincidence in the range of temperatures $T=0.05-1000$ for $N_p=11$ and in the range $T=0.2-1000$ for $N_p=81$.

In Figs. 5(a) and 5(b) one can see that there exist horizontal asymptotes at high and low temperatures. At $T\to0$, $E(T)/N_p$ tend to the specific energies of the ground states, which are close to each other for polyions of different lengths. The asymptotes at $T\to\infty$ are different for different N_p, and their values become higher with increasing polyion length. It is possible that high-temperature asymptotes tend to a certain limiting value at $N_p\to\infty$, though calculations for longer chains are required in order to clarify this possibility.

There exists another way, different from Eq. (4), to obtain the $E(T)$ dependency. If the distribution $\Omega(E)$ is known one can employ the microcanonical formula $\delta S/\delta E=1/T$. We computed $E(T)$ this way, by taking δS as the difference of entropies between neighboring energy states, $\delta S_i=\ln[\Omega(E_{i+1})]-\ln[\Omega(E_i)]$, and δE as the energy difference between them, $\delta E=E_{i+1}-E_i$. So for each E_i the corresponding $1/T_i$ value is calculated, and we get the dependency $E(T)$. In Fig. 6 a good coincidence is observed for $E(T)$ dependencies obtained according to these two approaches in a wide temperature range, $T=0.06-50$. It is seen that the data obtained

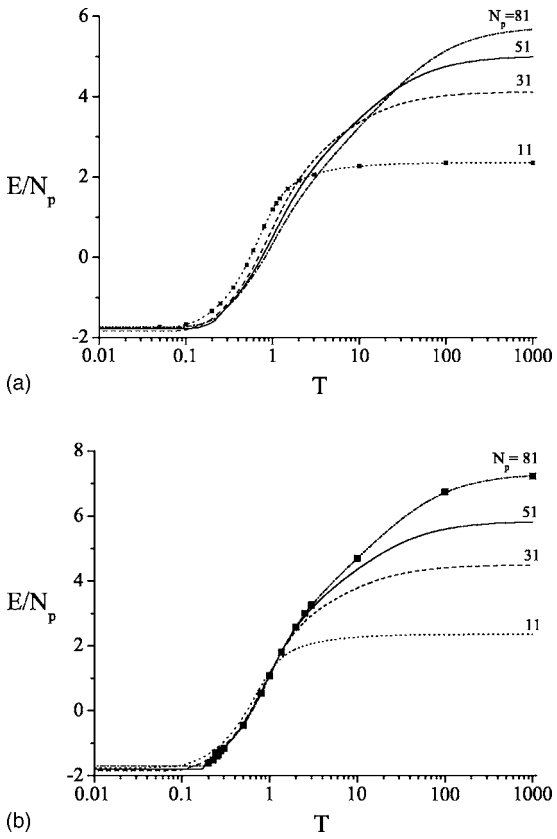

FIG. 5. Specific energies as functions of temperature for $N_p=11$ (dot line), 31 (dash line), 51 (solid line), and 81 (dash-dot line). Squares are results of Metropolis simulations. (a) First series of calculations (fixed side length of the cell) and (b) second series (fixed volume fraction per monomer).

by canonical averaging (4) are slightly higher than the results of numerical differentiation only in the high-temperature area. This depends on the fact that all energy states take part in determining $E(T)=\langle E\rangle_{\mathrm{can}}$, contrary to the latter approach where small energy intervals are used for calculating this

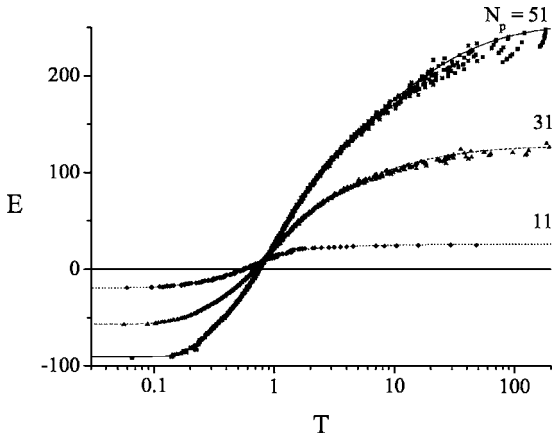

FIG. 6. Temperature dependencies for internal energies: $N_p=11$ (dot line and diamonds), 31 (dash line and triangles), and 51 (solid line and squares) computed for the first series of simulations. Curves are for the canonical averages [Eq. (2)] and signs are for the microcanonical values.

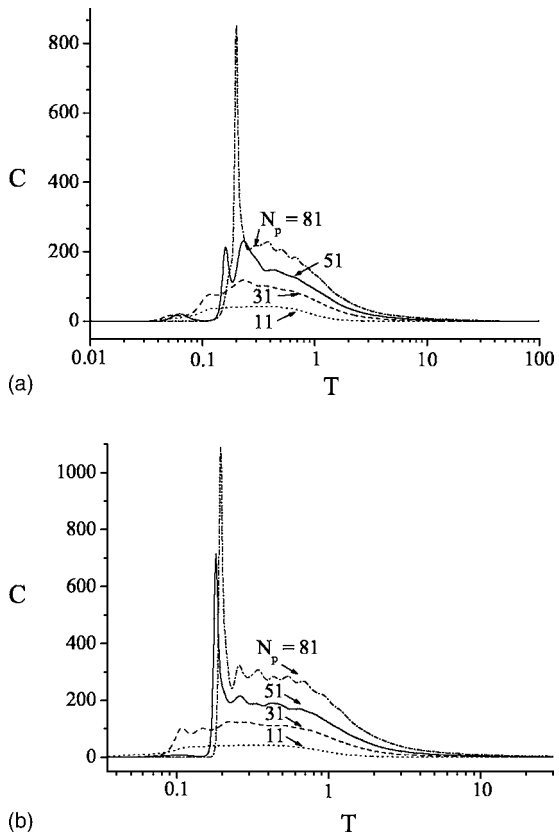

FIG. 7. Heat capacities as functions of T. Notations as in Fig. 5.

dependency. This is also related to a slight nonequivalence of the ensembles.

In Figs. 7(a) and 7(b) temperature dependencies of heat capacity are presented. For shorter chains, $N_p=11,31$, a relatively weak multimaxima shape of $C(T)$ dependencies is observed, while for longer chains, $N_p=51,81$, there emerge strong peaks which are most distinct for the second series of our data [Fig. 7(b)]. These narrow peaks might be considered as evidence of transition of the polyion to a closed globular conformation, which strongly resembles a second order phase transition. At low and high temperatures the $C(T)$ functions tend to zero. It is relevant here to point out the recent work of Rampf, Paul, and Binder [21], where the WL algorithm was applied to simulate a flexible noncharged polymer chain on a lattice. The obtained $C(T)$ dependencies for different chain lengths have a long high-temperature shoulder and a tall peak at its left side (Fig. 2 of [21]). Finite size scaling of the $C(T)$ maxima performed in that work indicates the existence of a two-stage transition for chains of finite length: Coil-globule and crystallization. Our $C(T)$ data, Fig. 7, have qualitatively the same character, i.e., a long high-temperature shoulder with a strong peak at its left side for $N_p=51,81$, Fig. 7(b). However, our data are yet insufficient to make a similar analysis and simulations of longer polyions are needed.

In Figs. 8(a) and 8(b) we present the temperature dependency of the canonical part of the free energy $\Delta F(T)$ (8) together with the energy $E(T)$ according to Eq. (4). It can be

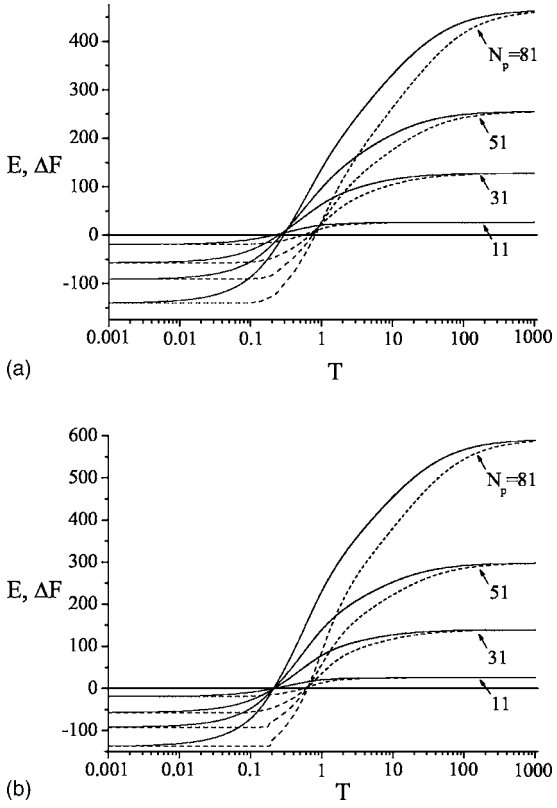

FIG. 8. Energies E (dash lines) and excess canonical free energies ΔF (solid lines) as functions ot T. (a) First series of calculations and (b) second series.

seen that $E(T)$ and $\Delta F(T)$ have the same asymptotes at $T\to 0$ and at $T\to\infty$ for each N_p. In order to understand this, consider first the case of low temperatures. In the expression (8) at $T\to 0$ we retain only significant terms:

$$\Delta F(T) \approx -T\ln\left[\exp\left(-\frac{E_1}{T}\right)\Omega_1\right] = -T\left(-\frac{E_1}{T}\right) - T\ln\Omega_1 \to E_1,$$

where $E_1 \equiv E_{\min}$ is the lowest energy (the ground state of the model) and $\Omega_1 \equiv \Omega(E_1)$. From the expression (4) one can see that for the energy at $T\to 0$

$$\langle E\rangle(T) \to \frac{E_1 \exp\left(-\frac{E_1}{T}\right)\Omega_1}{\exp\left(-\frac{E_1}{T}\right)\Omega_1} = E_1,$$

so both $E(T)$ and $\Delta F(T)$ tend to the energy of ground state E_1.

Considering another limit, $T\to\infty$, we use the expansion of the exponent in Eq. (8):

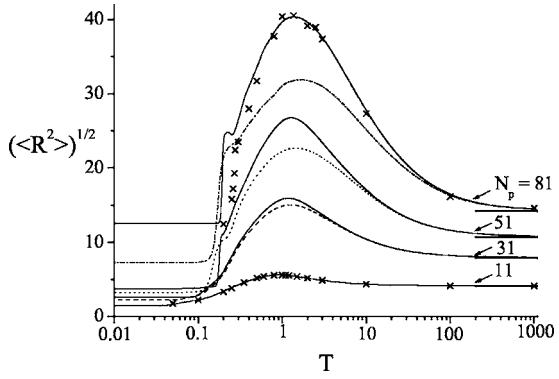

FIG. 9. Dependency of average end-to-end distance $\sqrt{\langle R^2\rangle}$ on temperature. First series of calculations (constant side length of the cell): $N_p=11$ (solid line), 31 (dash line), 51 (dot line), and 81 (dash-dot line). Second series of calculations is given by solid lines which approach corresponding lines of the first series at $T\to\infty$. Crosses denote Metropolis method data for $N_p=11$ and 81 for the second series of calculations. Horizontal lines at the right-hand side correspond to the scaling values $\sqrt{\langle R_N^2\rangle}=1.025\times N^{3/5}$, where $N=N_p-1$.

$$\Delta F(T) \approx -T\ln\sum_i\left(1-\frac{E_i}{T}\right)\Omega_i = -T\ln\left(1-\frac{1}{T}\sum_i E_i\Omega_i\right)$$

(because $\Sigma_i\Omega_i=1$). We expand the logarithm and finally obtain $\Delta F(T)\approx\Sigma_i E_i\Omega_i$. From the expression (4) we get for the energy at $T\to\infty$:

$$\langle E\rangle(T) \approx \frac{\sum_i E_i\Omega_i}{\sum_i \Omega_i} = \sum_i E_i\Omega_i.$$

A noticeable feature of the ΔF and E curves is that each pair of curves for different N intersects. It is striking that points of pairwise intersections are very close to each other both for E and ΔF. For the second series of data [Fig. 8(b)] it is clearly seen that all the curves pass through a single common point. For ΔF this point is $\Delta F\approx 0$, $T\approx 0.2$. This means that the excess canonical free energy of the system is almost independent on the polyion length at this temperature. Note also that strong peaks of the heat capacity, Fig. 7(b), are in the same temperature interval.

The obtained data for Ω_0, the fraction of nonoverlapping configurations, as well as corresponding entropy contributions, S_{at}, are given in Table I. We have also evaluated values of S_{at} from the scaling relations (14) and (15), which are given in Table I in column $S_{\text{at}}^{\text{scal}}$. One can see that the deviations of the MC data from analytical scaling results for ΔS_{at} are in the range (0.1–1)%, which confirms that overlapping configurations are accounted for in our approach in a proper way.

The dependencies of average end-to-end distance $\sqrt{\langle R^2\rangle}$ on temperature for both series of our data are presented in Fig. 9. The curves for all N_p have maxima in the neighborhood of $T\approx 1$. This feature is in agreement with the results obtained by the Metropolis method in our early work [2] and also with the results presented by Klos and Pacula in [6]. Locations and magnitudes of the maxima are collected in

Table I. The maxima are higher for the second series of data, and they increase faster with the growth of the polyion length. The effect is rather expected since, in the first series of simulations, the counterion concentration is increasing upon increase of the polyion length, which leads to higher screening and slower growth of the polyion coil. It can also be seen that the maximum of the curve $\sqrt{\langle R^2\rangle}(T)$ slightly shifts to higher temperatures with increasing polyion length, the effect being more pronounced in the first series of simulations. The general result is that at $T\approx 1$ the polyion is most expanded compared with its conformations at other temperatures, though the exact location of the temperature maximum depends on the polyion length and the monomer concentration.

At high temperatures $\sqrt{\langle R^2\rangle}$ should tend to the scaling value for the neutral self-avoiding chains in the athermal case, $\sqrt{\langle R_N^2\rangle}\propto N^{3/5}$, where $N=N_p-1$ (according to our estimations in [28] the proportionality coefficient in this expression equals 1.025). As seen in Fig. 9, our curves indeed asymptotically tend to these levels for both series of data.

At $T\ll 1$ the counterion condensation becomes very strong, leading to a pronounced decrease of the chain's size and transition to a globule. For $N_p=51,81$ this transition has the character of an abrupt jump at $T\sim 0.1-0.2$, which is especially pronounced for data of the second series. Together with results for the heat capacity [Figs. 7(a) and 7(b)] it can be treated as evidence for a phase transition of the system. Comparison with data, obtained by the standard MC method (Metropolis procedure) shows complete coincidence of the two approaches for $N_p=11$ within the whole range of T. For the longest polyion, $N_p=81$, good coincidence is obtained within a wide range of T. Only in the regime of collapse there is observed a noticeable discrepancy between the two data sets, although the qualitative behavior is similar also in this interval, $0.2\leq T\leq 0.5$. A possible reason for this disagreement is the existence of extended polyion conformations of low energy, which are poorly sampled (or are not sampled at all) in canonical simulations. We therefore consider the WL result in this temperature range as more reliable.

Experimentally, collapse of strongly charged polyelectrolytes is often observed when multivalent ions are added to the solution [38,39]. Note that the reduced temperature $T=1/\xi$ cannot change much due to a change of the real temperature in an experiment (taking into account that the dielectric constant decreases with the real temperature), but a substantial change of T can be reached by increasing the unit charge q, for example by substitution of monovalent ions by multivalent ones. For most of real polyelectrolytes parameter $\xi<5$, and the corresponding reduced temperature is above the phase transition point at $T\approx 0.2$. However, substitution of monovalent counterions by ions of valency Z leads to an effective Z-fold decrease of T, and many real polyelectrolytes fall into the region when collapse of a polyelectrolyte chain is possible.

IV. CONCLUSION

In this paper we extended our previous ES simulations of polymer models within the WL algorithm [28,29] applying it now to flexible polyelectrolytes. We considered a lattice model of a polyion surrounded by explicit mobile ions with Coulombic interactions and obtained energy distributions of nonoverlapped configurations. These distributions provide calculation of the internal energy, heat capacity, free energy, entropy, and mean square end-to-end distance in a wide range of temperatures by a simple one-dimensional integration. Calculations have been done for different polyion length and monomer concentrations.

The main advantage of the used scheme, as we see it, is that overlaps of chains are not rejected but are accounted for in a proper way. Certainly such an approach when parts of a chain are allowed to pass through each other can be used only in treatment of equilibrium properties and by no means are applicable in dynamics. However, in dynamical simulations of polymers they could be helpful in preparing a set of equilibrium initial configurations.

In studies of equilibrium athermal and thermal properties the ES-WL sampling schemes can be readily applied to more complicated models, e.g., flexible and semiflexible polyelectrolytes with the added salt, ring, branched, and anchored polyionic chains.

ACKNOWLEDGMENTS

The work has been supported by the Russian Foundation for Fundamental Research (RFFI), Grant No. 05-02-17428, and by the Swedish Royal Academy of Sciences.

[1] A. P. Lyubartsev and L. Nordenskiöld, *Handbook of Polyelectrolytes and Their Applications* (American Scientific Publishers, Los Angeles, 2002), Chap. 11, pp. 309–325.
[2] A. P. Lyubartsev and P. N. Vorontsov-Velyaminov, Vysokomol. Soedin., Ser. A **32**, 721 (1990).
[3] M. Severin, J. Chem. Phys. **99**, 628 (1993).
[4] M. J. Stevens and K. Kremer, J. Chem. Phys. **103**, 1669 (1995).
[5] M. J. Stevens and S. J. Plimpton, Eur. Phys. J. B **2**, 341 (1998).
[6] J. Klos and T. Pakula, J. Chem. Phys. **120**, 2496 (2004).
[7] J. Klos and T. Pakula, J. Chem. Phys. **120**, 2502 (2004).
[8] J. Klos and T. Pakula, J. Chem. Phys. **122**, 134908 (2005).
[9] P.-Y. Hsiao, J. Chem. Phys. **124**, 044904 (2006).
[10] A. P. Lyubartsev, A. A. Martsinovskii, S. V. Shevkunov, and P. N. Vorontsov-Velyaminov, J. Chem. Phys. **96**, 1776 (1992).
[11] B. A. Berg and T. Neuhaus, Phys. Rev. Lett. **68**, 9 (1992).
[12] J. Lee, Phys. Rev. Lett. **71**, 211 (1993).
[13] Y. Iba, Int. J. Mod. Phys. C **12**, 623 (2001).
[14] A. Mitsutake, Y. Sugita, and Y. Okamoto, Biopolymers **60**, 96 (2001).
[15] A. P. Lyubartsev and P. N. Vorontsov-Velyaminov, Recent Res.

Dev. Chem. Phys. **4**, 63 (2003).
[16] F. Wang and D. P. Landau, Phys. Rev. Lett. **86**, 2050 (2001).
[17] F. Wang and D. P. Landau, Phys. Rev. E **64**, 056101 (2001).
[18] Q. Yan, R. Faller, and J. J. de Pablo, J. Chem. Phys. **116**, 8745 (2002).
[19] M. S. Shell, P. G. Debenedetti, and A. Z. Panagiotopoulos, Phys. Rev. E **66**, 056703 (2002).
[20] R. Faller and J. J. de Pablo, J. Chem. Phys. **119**, 4405 (2003).
[21] F. Rampf, W. Paul, and K. Binder, Europhys. Lett. **70**, 628 (2005).
[22] N. Rathore and J. J. de Pablo, J. Chem. Phys. **116**, 7225 (2002).
[23] N. Rathore, T. A. Knotts, and J. J. de Pablo, J. Chem. Phys. **118**, 4285 (2003).
[24] N. Rathore, Q. Yan, and J. J. de Pablo, J. Chem. Phys. **120**, 5781 (2005).
[25] E. B. Kim, R. Faller, Q. Yan, N. L. Abbott, and J. J. de Pablo, J. Chem. Phys. **117**, 7781 (2002).
[26] F. Calvo, Mol. Phys. **100**, 3421 (2002).
[27] B. J. Schulz, K. Binder, and M. Muller, Int. J. Mod. Phys. C **13**, 477 (2002).
[28] P. N. Vorontsov-Velyaminov, N. A. Volkov, and A. A. Yurchenko, J. Phys. A **37**, 1573 (2004).
[29] N. A. Volkov, A. A. Yurchenko, A. P. Lyubartsev, and P. N. Vorontsov-Velyaminov, Macromol. Theory Simul. **14**, 491 (2005).
[30] J. Douglas, C. M. Guttman, A. Mah, and T. Ishinabe, Phys. Rev. E **55**, 738 (1997).
[31] P. Grassberger and R. Hegger, J. Chem. Phys. **102**, 6881 (1995).
[32] P. Ewald, Ann. Phys. **64**, 253 (1921).
[33] M. P. Allen and D. J. Tildesley, *Computer Simulations of Liquids*, 2nd ed. (Clarendon, Oxford, 1987).
[34] P. H. Hunenberger and J. A. McCammon, J. Chem. Phys. **110**, 1856 (1999).
[35] A. Tröster and C. Dellago, Phys. Rev. E **71**, 066705 (2005).
[36] P. G. de Gennes, *Scaling Concepts in Polymer Science* (Cornell University Press, Ithaca and London, 1979).
[37] D. Zhao, Y. Huang, Z. He, and R. Qian, J. Chem. Phys. **104**, 1672 (1996).
[38] M. O. de la Cruz, L. Belloni, M. Delsanti, J. P. Dalbiez, O. Spalla, and M. Drifford, J. Chem. Phys. **103**, 5781 (1995).
[39] T. Iwataki, S. Kidoaki, T. Sahaue, K. Yoshikawa, and S. S. Abramchuk, J. Chem. Phys. **120**, 4004 (2004).